J. Am. Soc. Mass Spectrom. (2013) 24:1523–1533
DOI: 10.1007/s13361-013-0689-7

RESEARCH ARTICLE

IRMPD Action Spectroscopy of Alkali Metal Cation–Cytosine Complexes: Effects of Alkali Metal Cation Size on Gas Phase Conformation

Bo Yang,[1] R. R. Wu,[1] N. C. Polfer,[2] G. Berden,[3] J. Oomens,[3,4] M. T. Rodgers[1]

[1]Department of Chemistry, Wayne State University, Detroit, MI 48202, USA
[2]Department of Chemistry, University of Florida, Gainesville, FL 32611, USA
[3]Institute for Molecules and Materials, FELIX Facility, Radboud University Nijmegen, Toernooiveld 7, 6525ED Nijmegen, The Netherlands
[4]van't Hoff Institute for Molecular Sciences, University of Amsterdam, Amsterdam, The Netherlands

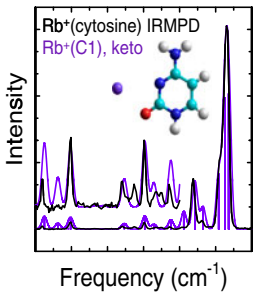

Abstract. The gas-phase structures of alkali metal cation-cytosine complexes generated by electrospray ionization are probed via infrared multiple photon dissociation (IRMPD) action spectroscopy and theoretical calculations. IRMPD action spectra of five alkali metal cation–cytosine complexes exhibit both similar and distinctive spectral features over the range of ~1000–1900 cm^{-1}. The IRMPD spectra of the Li^+(cytosine), Na^+(cytosine), and K^+(cytosine) complexes are relatively simple but exhibit changes in the shape and shifts in the positions of several bands that correlate with the size of the alkali metal cation. The IRMPD spectra of the Rb^+(cytosine) and Cs^+(cytosine) complexes are much richer as distinctive new IR bands are observed, and the positions of several bands continue to shift in relation to the size of the metal cation. The measured IRMPD spectra are compared to linear IR spectra of stable low-energy tautomeric conformations calculated at the B3LYP/def2-TZVPPD level of theory to identify the conformations accessed in the experiments. These comparisons suggest that the evolution in the features in the IRMPD action spectra with the size of the metal cation, and the appearance of new bands for the larger metal cations, are the result of the variations in the intensities at which these complexes can be generated and the strength of the alkali metal cation-cytosine binding interaction, not the presence of multiple tautomeric conformations. Only a single tautomeric conformation is accessed for all five alkali metal cation–cytosine complexes, where the alkali metal cation binds to the O2 and N3 atoms of the canonical amino-oxo tautomer of cytosine, $M^+(C_1)$.

Key words: Alkali metal cations, Cytosine, Gas-phase conformations, Infrared multiple photon dissociation action spectroscopy, Tautomers

Received: 5 April 2013/Revised: 1 June 2013/Accepted: 3 June 2013/Published online: 27 July 2013

Introduction

According to the central dogma of molecular biology, the genetic information stored in double-stranded DNA (dsDNA) is duplicated via production of two identical copies of the molecule. At the first step of replication, DNA polymerase recognizes a single nucleobase [adenine (A), thymine (T), cytosine (C), or guanine (G)] of the template strand from the original dsDNA. The complementary nucleobase (A*=T, T*=A, C*=G, and G*=C) is then recruited from the local environment to correctly pair the original base with the complementary base by two (A::T) or three (C:::G) hydrogen bonds. A new dsDNA is synthesized from an existing single-stranded DNA (ssDNA) template by successfully pairing all nucleobases. Clearly, base–base recognition and, hence, proper base pairing are crucial to successful DNA replication [1]. However, the nucleobases can exist in several tautomeric states that lie close in energy, and the tautomeric equilibria among these states can be sensitive to the local environment. Experiments have established that metal cation binding to the nucleobases can lead to formation of rare

Electronic supplementary material The online version of this article (doi:10.1007/s13361-013-0689-7) contains supplementary material, which is available to authorized users.

Correspondence to: M. T. Rodgers; *e-mail:* mrodgers@chem.wayne.edu

tautomers of the nucleobases [2–11]. In many cases, rare tautomers exhibit different hydrogen bonding characteristics such that their presence may induce formation of mismatched base pairs and lead to gene mutation [12, 13]. Tautomerization of the nucleobases at any stage of the replication process may alter the sequence or structure of the newly-formed dsDNA. Therefore, comprehensive studies of the interactions between metal cations and isolated nucleobases in the gas phase are necessary to elucidate the effects of metal cation binding on the tautomeric states and stabilities of the nucleobases so as to understand the roles that metal cations play in biological systems and their influence on DNA replication processes.

Previously, theoretical studies [14–31] have examined all possible tautomers of isolated cytosine and found that six lie relatively low in energy. The structures of these six low-energy tautomers of cytosine, including the canonical tautomer of cytosine, C_1, found in DNA, are shown in Figure S1 of the Supplementary Information. However, IR matrix isolation [32] and microwave spectroscopy [33] studies as well as theoretical studies of the unimolecular and bimolecular tautomerization of cytosine suggest that only the C_1, C_2, and C_4 tautomers are generated upon thermal vaporization of cytosine.

Ab initio calculations have been performed by Monajjemi et al. [30] on the M^+(cytosine) complexes, where M^+=Li^+, Na^+, K^+, Rb^+, and Cs^+, to examine the influence of N4 metalation on the tautomeric equilibria of cytosine. Their results indicate that binding of alkali metal cations to the exocyclic amino group of cytosine induces protonation of a nucleobase ring nitrogen atom and, hence, causes a proton shift from an exocyclic to an endocyclic nitrogen atom, leading to the generation of rare nucleobase tautomers, C_4 and C_5 [34]. The roles that coordinated metal cations can play in stabilizing or generating minor tautomers of the nucleobases upon binding have been evaluated theoretically, and the results have recently been reviewed by Lippert and Gupta [35]. Metal cation binding to other sites of cytosine may either stabilize a rare tautomer or lead to the generation of a rare tautomer via binding to the major tautomer followed by a proton transfer reaction. However, in most cases, the metal catalyzed stabilization of rare tautomers predicted by theory still awaits experimental validation. Recently, noncovalent interactions of cytosine with the alkali metal cations, Li^+, Na^+, and K^+, were studied using guided ion beam tandem mass spectrometry techniques, where the M^+(cytosine) complexes were generated by gas-phase three-body condensation in a flow tube ion source [11]. Based upon the measured thresholds for collision-induced dissociation (CID) of the M^+(cytosine) complexes and calculated bond dissociation energies (BDEs) as well as the barriers to tautomerization for the low-energy tautomeric forms of M^+(cytosine), it was concluded that tautomerization occurs during both gas-phase complex formation and CID [11].

In the case of M^+(cytosine) complexes, where M^+=Li^+, Na^+, and K^+, both the ground-state $M^+(C_1)$ structure and excited $M^+(C_3)$ tautomeric conformations were accessed when the complexes were generated by gas-phase condensation of dc discharge generated alkali metal cations and thermally vaporized cytosine. However, the measured thresholds do not actually probe the binding in the ground-state $M^+(C_1)$ structures and, thus, it will be useful to re-examine these systems under conditions where only the ground-state $M^+(C_1)$ complexes are generated, possibly by electrospray ionization (ESI). Thus, part of the motivation for the current work is to determine whether ESI produces only the ground-state $M^+(C_1)$ conformers, or if excited conformations are also accessed as observed for M^+(cytosine) complexes generated by gas phase condensation of the alkali metal cation and thermally vaporized cytosine [11]. Rb^+ and Cs^+ cations share chemical similarity with K^+, and are found to replace K^+, causing potassium deficiency [36]. Given these observations, it is of interest to explore the conformations of metal cationized cytosine to the heavier alkali metal cations, Rb^+ and Cs^+ as well. In the present work, we use infrared multiple photon dissociation (IRMPD) action spectroscopy to characterize the tautomeric conformations of the M^+(cytosine) complexes generated by ESI and to determine how they are influenced by the size of the alkali metal cation. Identification of the conformations present is achieved by comparison of the measured IRMPD spectra to linear IR spectra derived from electronic structure calculations of the stable low-energy tautomeric conformations of the M^+(cytosine) complexes determined at the B3LYP/def2-TZVPPD level of theory.

Experimental and Computational

Mass Spectrometry and Photodissociation

IRMPD action spectra of five M^+(cytosine) complexes, where M^+=Li^+, Na^+, K^+, Rb^+, and Cs^+, were measured using a 4.7 T Fourier transform ion cyclotron resonance mass spectrometer (FT-ICR MS) coupled to a free electron laser (FEL) source that was housed at the FOM Institute for Plasma Physics, Rijnhuizen, and has been described in detail elsewhere, but has recently been moved to the Radboud University of Nijmegen [37–39]. The alkali metal cation–cytosine complexes were generated using a Micromass "Z-spray" electrospray ionization (ESI) source from solutions containing 0.1–0.5 mM cytosine and 0.1–0.5 mM alkali metal chloride or alkali metal hydroxide in an approximately 50 %:50 % MeOH:H_2O mixture. All of the alkali metal chloride or alkali metal hydroxide samples were obtained from Sigma-Aldrich (Zwijndrecht, The Netherlands). Cytosine was purchased from Fluka (Zwijndrecht, The Netherlands). A solution flow rate of 10–30 μL/min was used and the ESI needle was generally held at a voltage of ~3 kV. Ions emanating from the ESI source were accumulated in a hexapole trap for 4 to 5 s followed by pulsed extraction through a quadrupole bender and injection into the ICR cell by an rf octopole ion guide. The precursor ions were mass selected using stored waveform inverse Fourier transform

(SWIFT) techniques and irradiated by the FEL at pulse energies of ~40 mJ per macropulse of 5 μs duration for 2–3 s, corresponding to interaction with 10 to 15 macropulses over the wavelength range extending from 10.0 μm (1000 cm^{-1}) to 5.5 μm (1820 cm^{-1}) for the complexes to Li^+, Na^+, and K^+, and from 17.4 μm (575 cm^{-1}) to 5.3 μm (1887 cm^{-1}) for the complexes to Rb^+ and Cs^+. No dissociation of the Li^+(cytosine), Na^+(cytosine) and K^+(cytosine) complexes was observed below 1000 cm^{-1}, which is likely the result of the weaker intensities at which these complexes could be generated and the larger number of photons needed to induced dissociation at these frequencies, and thus data were not acquired below 1000 cm^{-1} for these complexes.

Computational Details

In previous work, Yang and Rodgers [11] examined the low-energy tautomeric conformations of cytosine and its complexes with Li^+, Na^+, and K^+ as well as the transition states for unimolecular tautomerization of these complexes by ab initio calculations using Gaussian 03 [40]. Briefly, geometry optimizations and vibrational analyses were performed at the MP2(full)/6-31G* level. Single point energy calculations were performed at the MP2(full)/6-311+G(2d,2p) level of theory using the MP2(full)/6-31G* optimized geometries. Vibrational frequencies were scaled by a factor of 0.9646 for zero point energy (ZPE) corrections [41, 42]. In the present study, geometry optimizations and vibrational frequency analyses of five alkali metal cation–cytosine complexes with the six low-energy tautomers of cytosine were carried out using Gaussian 09 [43] at the B3LYP/6-31G*, MP2(full)/6-31G*, B3LYP/def2-TZVPPD, and MP2(full)/def2-TZVPPD levels of theory. The def2-TZVPPD basis set [44] is a balanced basis set on all atoms at the triple zeta level including polarization and diffuse functions [45]. The def2-TZVPPD basis set was obtained from the EMSL basis set exchange library [46, 47]. These levels of theory have been shown to provide reasonably accurate structural and energetic descriptions of comparable metal-ligand systems [48]. Single point energy calculations of the stable low-energy conformations were performed using the extended 6-311+G(2d,2p) [49] basis set at the B3LYP and MP2(full) levels of theory, while the energetics for the calculations using the def2-TZVPPD basis set were used directly. Zero point energy (ZPE) corrections were determined using vibrational frequencies calculated at the B3LYP and MP2(full) levels scaled by a factor of 0.9804 and 0.9646 [41, 42], respectively.

For the Rb^+ and Cs^+ complexes, all conformations considered previously for K^+(cytosine), were used as starting points for geometry optimizations and vibrational frequency analyses at all four levels of theory, MP2(full)/6-31G*_HW*, B3LYP/6-31G*_ HW*, B3LYP/def2-TZVPPD, and MP2(full)/def2-TZVPPD, where HW* indicates that Rb and Cs were described using the effective core potentials (ECPs) and valence basis sets of Hay and Wadt [50] with a single d polarization function (with exponents of 0.24 and 0.19, respectively) included [51]. The calculations that make use of the def2-TZVPPD basis set utilize the ECPs developed by Leininger et al. for Rb^+ and Cs^+ [45]. Energetics are determined from single point energies computed at the analogous levels of theory.

IR spectra were generated from the computed vibrational frequencies and Raman intensities using the harmonic oscillator approximation and analytical derivatives of the energy-minimized Hessian calculated at the B3LYP/def2-TZVPPD level of theory. Frequencies were scaled by 0.98 for the M^+(cytosine) complexes, where M^+=Na^+, K^+, Rb^+, and Cs^+, and by 0.97 for the Li^+(cytosine) complex to eliminate known systematic error [41]. A smaller scaling factor is used for the Li^+(cytosine) complex because previous studies have shown that theory underestimates the strength of binding in Li^+(ligand) complexes [52], which results in less red-shifting of spectral features involved in the alkali-metal cation binding interaction. For comparison to experiment, calculated vibrational frequencies are broadened using a 20 cm^{-1} full width at half maximum (FWHM) Gaussian line shape.

Results and Discussion

IRMPD Action Spectroscopy

Photodissociation of the M^+(cytosine) complexes, where M^+= Na^+, K^+, Rb^+, and Cs^+, leads to loss of intact neutral cytosine and detection of the alkali metal cation for all four complexes, consistent with CID results for the complexes to Li^+, Na^+, and K^+ [11]. For the Li^+(cytosine) complex, the Li^+ cation is too light to be detected efficiently, thus the IRMPD spectrum of the Li^+(cytosine) complex is plotted as an inverted depletion spectrum, where the signal of the Li^+(cytosine) complex is monitored and inverted. No fragments were observed, suggesting that Li^+ is the only ionic product formed upon IRMPD, consistent with CID results. For the other four alkali metal cation–cytosine complexes, the IRMPD action spectra are plotted as the IRMPD yield of the M^+ product cation as a function of wavelength, as shown in Figure 1. An IRMPD yield was determined from the precursor ion intensity (I_p) and the M^+ fragment ion intensity (I_f) after laser irradiation at each frequency as shown in Equation (1)

$$\text{IRMPD yield} = I_f/(I_p + I_f) \quad (1)$$

The IRMPD yield (signal for the Li^+(cytosine) complex) was normalized linearly with laser power to correct for changes in the laser power as a function of the photon energy (i.e., the wavelength of the FEL).

The IRMPD spectrum of the Li^+(cytosine) complex exhibits two broad bands at 1480 and 1635 cm^{-1}. Comparison of the spectra in Figure 1 shows that the IR features observed in the Li^+(cytosine) spectrum are retained for all five alkali metal cation–cytosine complexes, but that new IR

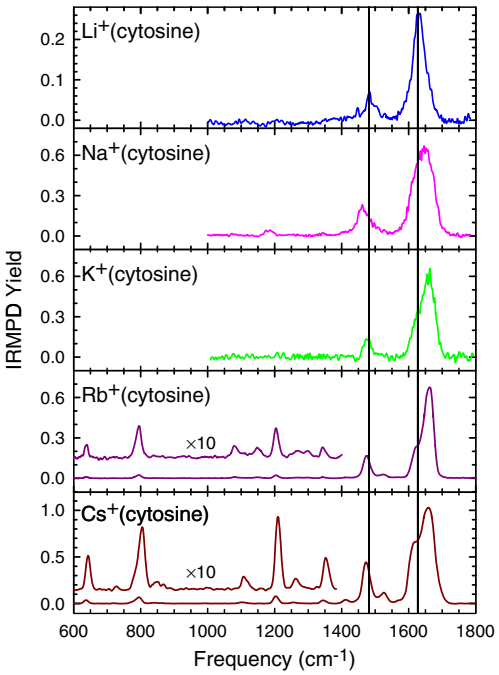

Figure 1. IRMPD action spectra of M^+(cytosine) complexes, where M^+=Li^+, Na^+, K^+, Rb^+, and Cs^+

bands begin to emerge for the Na^+(cytosine) complex, and become obvious for the Rb^+(cytosine) and Cs^+(cytosine) complexes. The noncovalent interactions between the alkali metal cation and cytosine are weaker for the larger alkali metal cations, Rb^+ and Cs^+; therefore, it is easier to fragment the Rb^+(cytosine) and Cs^+(cytosine) complexes, leading to higher yields. The IRMPD yield is fairly constant for the complexes to Na^+, K^+, and Rb^+, and increases by nearly a factor of two for the complex to Cs^+. However, it is clear that the signal to noise has markedly improved for the Rb^+ and Cs^+ cations as a result of the much greater intensity at which these species are generated by ESI. The B3LYP/def2-TZVPPD alkali metal cation-cytosine binding affinities of cytosine are 285.1, 215.1, 161.4, 143.3, and 131.8 kJ/mol for Li^+, Na^+, K^+, Rb^+, and Cs^+, respectively. In addition, the ion intensities of the M^+(cytosine) complexes that could be generated by ESI exhibit an inverse correlation with the strength of binding such that the signal to noise ratio (S/N) of the spectra for the larger alkali metal cation-cytosine complexes is much better than that for the complexes to the smaller alkali metal cations, Li^+, Na^+, and K^+. The most intense band for the Li^+(cytosine) complex appears at ~1635 cm^{-1} and is fairly symmetric. As the size of the alkali metal cation increases from Na^+ to Cs^+, this band becomes increasingly asymmetric, and eventually exhibits an obvious shoulder to the red of the main band for the Rb^+(cytosine) and Cs^+(cytosine) complexes, suggesting that more than one mode contributes to this feature. The band at 1480 cm^{-1} in the spectrum of the Li^+(cytosine) complex is increasingly red-shifted in the IRMPD spectra of the complexes to K^+, Rb^+, and Cs^+. However, the Na^+(cytosine) complex exhibits somewhat anomalous behavior in that this band is the most red-shift for Na^+. Subtle differences that evolve for the complexes to the largest alkali metal cations, Rb^+ and Cs^+, include a rise in the intensity of several bands below 1400 cm^{-1} that now make these features discernable from noise, whereas no discernable dissociation of the complexes to the smaller alkali metal cations was observed below 1000 cm^{-1}. Thus, the spectra for these two latter complexes were measured down to 600 cm^{-1}. In particular, bands are now observed at approximately 640, 790–800, 1080–1110, 1210, 1270, and 1350 cm^{-1} in addition to the feature at approximately 1530 cm^{-1}.

Theoretical Results

A detailed discussion of the tautomeric structures of cytosine and its complexes with Li^+, Na^+, and K^+ can be found elsewhere [11]. As described above, the M^+(cytosine) complexes were calculated at B3LYP/6-311+G(2d,2p)_HW*, B3LYP/def2-TZVPPD, MP2(full)/ 6-311+G(2d,2p)_HW*, and MP2(full)/def2-TZVPPD levels of theory. The optimized structures obtained for the Rb^+(cytosine) complex of the six low-energy cytosine tautomers are shown in Figure 2. Similar structures are obtained for all of the M^+(cytosine) complexes, and are consistent with the structures obtained by Yang et al. [11]. Relative free energies at 298 K of these tautomeric

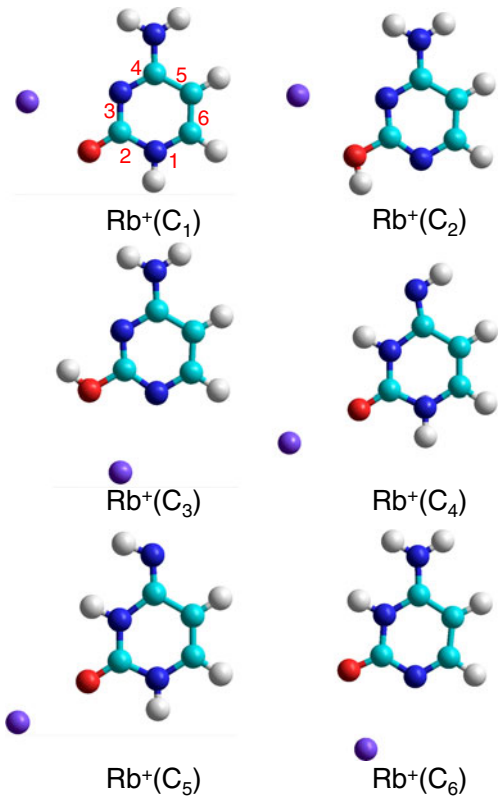

Figure 2. B3LYP/def2-TZVPPD optimized geometries of the most stable Rb^+ binding modes to each of the six low-energy tautomers of cytosine

conformations including ZPE corrections calculated at each level of theory for both neutral cytosine and the M^+(cytosine) complexes are given in Table 1. The MP2(full)/6-31G* results for Li^+(cytosine), Na^+(cytosine), and K^+(cytosine) calculated by Yang et al. [11] are also included in Table 1. Based on reports in the literature, the B3LYP/def2-TZVPPD basis set provides accurate energetics for similar alkali metal cation-ligand complexes [48, 53]. Thus, the B3LYP/def2-TZVPPD values are used throughout the following discussion except as noted. The calculations indicate that the preferred binding sites for all five alkali metal cations to the low-energy cytosine tautomers involve bidentate binding to the carbonyl oxygen and N3 ring nitrogen atoms (O2N3) for C_1 and C_2, bidentate binding to the N1 ring nitrogen and carbonyl oxygen atoms (N1O2) for C_3 and C_6, and monodentate binding to the carbonyl oxygen atom (O2) for C_4 and C_5, as shown in Figure 3 for the Rb^+(cytosine) complex.

In all cases, the most stable structure of the alkali metal cation cytosine complexes is the $M^+(C_1)$ tautomeric conformation shown in Figure 2, where the alkali metal cation binds to the O2 and N3 atoms of the canonical amino-oxo tautomer of cytosine. B3LYP results suggest that the amino-oxo tautomer, C_1, is also the most stable tautomeric form of isolated cytosine. We note that the M^+–O2 and M^+–N3 distances increase from 1.87 to 2.81 Å and 2.09 to 3.63 Å, respectively, as the alkali metal cation size increases from Li^+ to Cs^+. These changes directly reflect the increase in the ionic radius of the alkali metal cation (0.70 Å for Li^+, 0.98 Å for Na^+, 1.33 Å for K^+, 1.49 Å for Rb^+, and 1.69 Å for Cs^+) [54], which leads to longer alkali metal cation-cytosine bond distances and, therefore, weaker electrostatic interactions with cytosine. Interestingly, $M^+(C_6)$ is the next most stable tautomeric conformation, and lies 16.7–20.1 kJ/mol higher in Gibbs free energy than the ground-state structure, whereas in isolated cytosine, the C_6 tautomer is the least stable structure among the six low-energy tautomers and lies 30.6 kJ/mol above the ground-state C_1 conformer, indicating that the binding of alkali metal cation stabilizes this tautomeric conformation by ~10 −15 kJ/mol. The third most stable tautomeric conformation is the $M^+(C_3)$ complex, which lies between 47.9 and 38.7 kJ/mol higher in free energy than the ground-state $M^+(C_1)$ complex to Li^+–Cs^+, respectively. For the $M^+(C_3)$ complex, the alkali metal cation is bound to the N1 and O2 atoms, with the O2 hydrogen atom oriented toward the adjacent N3 atom. Rotation

Table 1. Relative Gibbs Free Energies of Neutral Cytosine and Alkali Metal Cation–Cytosine Complexes at 298 K in kJ/mol[a]

System	B3LYP/6-311+G(2d,2p)_HW*	MP2(full)/6-311+G(2d,2p)_HW*	B3LYP/def2-TZVPPD	MP2(full)/def2-TZVPPD
C_1	0.0	5.5	0.0	0.8
C_2	3.9	0.0	6.9	0.0
C_3	6.9	2.9	10.0	3.1
C_4	9.6	12.4	12.0	10.1
C_5	16.3	19.8	19.0	17.5
C_6	28.5	35.0	30.6	33.0
$Li^+(C_1)$	0.0	0.0[b]	0.0	0.0
$Li^+(C_2)$	64.7	54.1[b]	65.9	66.1
$Li^+(C_3)$	47.3	37.0[b]	48.0	49.1
$Li^+(C_4)$	81.7	83.6[b]	80.4	81.4
$Li^+(C_5)$	96.5	98.9[b]	95.2	98.1
$Li^+(C_6)$	18.5	21.2[b]	19.3	21.8
$Na^+(C_1)$	0.0	0.0[b]	0.0	0.0
$Na^+(C_2)$	56.0	44.5[b]	57.9	54.8
$Na^+(C_3)$	39.0	27.6[b]	40.5	40.1
$Na^+(C_4)$	73.9	74.4[b]	73.5	71.4
$Na^+(C_5)$	88.9	89.4[b]	88.3	87.8
$Na^+(C_6)$	16.7	19.1[b]	16.7	19.4
$K^+(C_1)$	0.0	0.0[b]	0.0	0.0
$K^+(C_2)$	51.5	37.9[b]	51.9	52.1
$K^+(C_3)$	35.5	22.5[b]	36.3	34.8
$K^+(C_4)$	62.4	63.6[b]	61.3	60.2
$K^+(C_5)$	76.9	78.3[b]	75.8	76.2
$K^+(C_6)$	17.2	18.6[b]	17.3	19.8
$Rb^+(C_1)$	0.0	0.0	0.0	0.0
$Rb^+(C_2)$	52.0	47.7	49.2	47.2
$Rb^+(C_3)$	34.9	30.0	35.0	33.3
$Rb^+(C_4)$	63.1	58.1	57.7	56.0
$Rb^+(C_5)$	78.6	73.9	72.0	71.9
$Rb^+(C_6)$	15.3	23.2	18.0	21.4
$Cs^+(C_1)$	0.0	0.0	0.0	0.0
$Cs^+(C_2)$	50.1	43.2	49.5	46.8
$Cs^+(C_3)$	33.7	22.4	36.4	34.3
$Cs^+(C_4)$	58.3	50.1	56.8	55.3
$Cs^+(C_5)$	73.2	65.7	71.0	70.9
$Cs^+(C_6)$	15.9	20.4	20.1	23.9

[a]Determined at the indicated level of theory including ZPE corrections
[b]Values taken from Reference 11

about the C2–O2 bond by 180° leads to a less stable tautomeric conformation, the $M^+(C_2)$ complex, which lies 65.9 to 51.9 kJ/mol higher in Gibbs free energies than the ground-state structure, respectively. In contrast to that found for the C_6 tautomer, alkali metal cation binding to the C_2 and C_3 tautomers significantly destabilize these tautomeric conformations (by ~45−59 kJ/mol and ~29−38 kJ/mol) as the C_2 and C_3 tautomers of isolated cytosine are computed to lie only 6.9 and 10.0 kJ/mol in Gibbs free energy above the ground-state C_1 tautomer, respectively. In the previous four tautomeric conformations (C_1, C_2, C_3, and C_6), the alkali metal cations are chelated with both oxygen and nitrogen atoms, leading to greater stabilization. When cytosine is in its imino-oxo tautomer, the alkali metal cation binds via interaction with the O2 carbonyl atom. The lack of chelation results in weaker binding, and, therefore, the tautomeric conformations, $M^+(C_4)$ and $M^+(C_5)$, are the least stable among the six low-energy tautomeric conformations. For the $M^+(C_4)$ complex, the N4 hydrogen atom is oriented away from the adjacent N3 atom. The $M^+(C_4)$ complexes lie between 80.4 and 56.8 kJ/mol higher in free energy for Li^+–Cs^+, respectively. Rotation about the C4–N4 bond by 180° produces the least stable tautomeric conformation, the $M^+(C_5)$ complexes, which lie 95.2 to 71.0 kJ/mol higher in Gibbs free energies than the analogous ground-state $M^+(C_1)$ complexes. Again, alkali metal cation binding to the C_4 and C_5 conformers significantly destabilizes these tautomers (by ~45−68 kJ/mol and 52−76 kJ/mol) as these tautomers of isolated cytosine are computed to lie only 12.0 and 19.0 in Gibbs free energy above the ground-state C_1 tautomer, respectively.

The variation in the relative Gibbs free energies of the stable low-energy tautomeric conformations of the M^+(cytosine) complexes as a function of the alkali metal cation is shown in Figure 3. For all five alkali metal cations, the relative Gibbs free energies of the M^+(cytosine) complexes follow the order: $M^+(C_1)<M^+(C_6)<M^+(C_3)<M^+(C_2)<M^+(C_4)<M^+(C_5)$, indicating that $M^+(C_1)$ is the most stable tautomeric conformation, whereas $M^+(C_5)$ is the least stable. This stability order differs from that found for isolated cytosine using density functional theory (DFT) where C_1 is found to be the most stable tautomeric conformation, whereas C_6 is the least stable, $C_1>C_2>C_3>C_4>C_5>C_6$ [14–31]. Calculations at the MP2(full) level of theory produce a different ordering of the stabilities of the low-energy tautomeric conformations of cytosine and indicate that the amino-hydroxy forms, C_2 and C_3, are global minima or near global minimum structures, while C_1 lies 5.9 kJ/mol higher in free energy. In contrast, the relative energies of the six low-energy tautomeric conformations of the M^+(cytosine) complexes follow the same order regardless of the level of theory used. The differences in the relative stabilities between the ground and excited tautomeric conformations generally decrease slightly as the size of the alkali metal cation increases, except there is a slight increase from Rb^+ to Cs^+ for the $M^+(C_2)$ and $M^+(C_3)$ tautomeric conformations. However, the $M^+(C_6)$ conformers exhibit nearly constant relative stability for the small alkali metal cations, Li^+, Na^+, and K^+, and then becomes increasingly less stable as the size of the alkali metal cation increases. However, even the first excited tautomeric conformation lies high enough in free energy above the ground-state $M^+(C_1)$ tautomeric conformation that it is unlikely to be produced in measurable abundance at room temperature, assuming that ESI produces an equilibrium distribution and that the computed energetics are reliable.

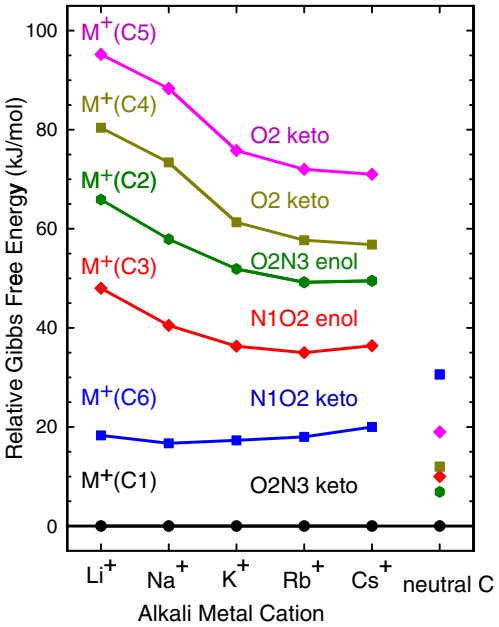

Figure 3. Relative Gibbs free energies at 298 K (kJ/mol) calculated at the B3LYP/def2-TZVPPD level of theory of the six most stable tautomeric conformations of the M^+(cytosine) complexes as a function of the alkali metal cation identity and of neutral cytosine

Comparison of IRMPD and Theoretical IR Spectra of Li^+(cytosine)

Figure 4 shows the experimental IRMPD action spectrum as well as the calculated linear IR spectra for the three most stable tautomeric conformations found for the Li^+(cytosine) complex. The calculated IR spectrum of the $Li^+(C_1)$ tautomeric conformation exhibits very good agreement with the observed action spectrum. All experimental bands have comparable theoretical frequencies and intensities, confirming that the ground-state structure is the dominant tautomeric conformation accessed in the experiments. The band observed at 1635 cm^{-1} corresponds to the carbonyl stretch, which explains its high intensity. Overlap of the carbonyl stretching mode with NH_2 scissoring at ~1610 cm^{-1} and the combination mode at ~1650 cm^{-1} arising from coupling of the carbonyl stretch, NH_2 scissoring, and N1−H wagging results in the single broad band in this region. The chelating interaction with the lithium cation leads to a redshift of this band compared with that for free cytosine, calculated at 1720 cm^{-1} at the B3LYP

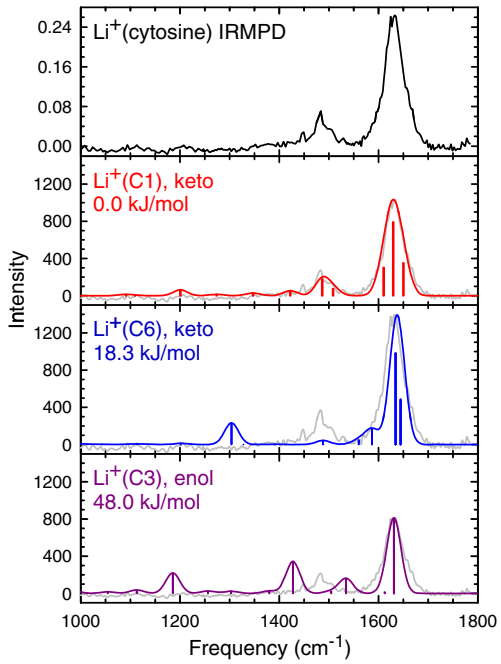

Figure 4. Comparison of the measured IRMPD action spectrum of the Li^+(cytosine) complex with IR spectra for the three most stable tautomeric conformations of Li^+(cytosine) predicted at the B3LYP/def2-TZVPPD level of theory. For ease of comparison, the IRMPD spectrum, scaled to match the intensity of the most intense spectral feature, is also shown in gray along with each of the theoretical IR spectra

level of theory. The experimentally observed band at 1480 cm^{-1} is the most diagnostic feature of the $M^+(C_1)$ conformation, and arises from the overlap of two modes arising from C4–N4 and N3–C4–C5 stretching. The position and the relative intensity of this band are in very good agreement with theoretical predictions. No other conformations are predicted to have an IR feature at this frequency. Optimistically, the weak bands predicted at 1091, 1201, 1347, and 1422 cm^{-1} also seem consistent with the measured IRMPD spectrum in this region. However, these bands are very weak, such that their magnitudes barely exceed the noise level in the data and, thus, cannot be reliably used to confirm the presence of the $Li^+(C_1)$ conformation in the experiments.

Comparison of the calculated IR spectrum of the first excited tautomeric conformation, $Li^+(C_6)$, to the IRMPD action spectrum suggests that the $Li^+(C_6)$ is not accessed in the experiments as there are several notable differences. The predicted CO stretch is slightly blueshifted to 1635 cm^{-1}, but becomes narrower compared with the measured IRMPD band at that frequency. The moderately intense band predicted to occur at 1304 cm^{-1} is not observed in the measured IRMPD spectrum. The weak IR features measured at 1210, 1360, and 1440 cm^{-1} do not appear in the predicted spectrum, but again their intensities in the calculated spectrum are sufficiently small that they cannot be reliably used to confirm the presence or absence of the $Li^+(C_6)$ conformation in the experiments. The calculated IR spectrum for the $Li^+(C_3)$ tautomeric conformation exhibits a strong band at 1631 cm^{-1} that corresponds to NH_2 scissoring coupled with C2–N3 and C5–C6 stretching, which agrees reasonably well with the most intense band measured at 1635 cm^{-1}. However, redshifting of the predicted CO stretch compared with the measured IRMPD band is much more pronounced because its functionality has changed from keto to enol such that it now appears at 1428 cm^{-1}, which does not have a comparable experimentally observed band. The calculations predict IR bands at 1534 and 1186 cm^{-1}, whereas no bands are observed at these frequencies in the measured IRMPD spectrum. Based on these differences, it is clear that the $Li^+(C_3)$ conformation is also not accessed in the experiments. Thus, the experimental IRMPD spectrum is well represented by that calculated for the ground-state $Li^+(C_1)$ tautomeric conformation; no evidence for the presence of excited tautomeric conformations in the experiments is observed.

Comparison of IRMPD and Theoretical IR Spectra of Na^+(cytosine)

As can be seen in Figure 2, the IRMPD spectral features of the Na^+(cytosine) complex are similar to those of the Li^+(cytosine) complex. Subtle differences include broadening and a 10 cm^{-1} blueshift of the most intense peak from ~1640 to 1650 cm^{-1}, and a 20 cm^{-1} redshift in the band at 1480 to 1460 cm^{-1}. Comparison of the measured IRMPD and theoretical linear IR spectra for the three most stable tautomeric conformations found for the Na^+(cytosine) complex is shown in the Supplementary Information, Figure S2. The calculated spectrum correctly predicts a 10 cm^{-1} blueshift in the band at 1640 cm^{-1}, and a 10 cm^{-1} redshift in the band at 1500 cm^{-1} as the metal cation changes from Li^+ to Na^+. The very weak bands at 1180, 1360, and 1430 cm^{-1} observed in the IRMPD action spectrum are also correctly predicted by calculations for the $Na^+(C_1)$ tautomeric conformation. It might also be noted that the two major peaks centered at 1640 and 1460 cm^{-1} in the measured IRMPD spectrum are broadened due to the redshift of the band predicted at ~1620 cm^{-1}, the blueshift of the bands predicted at ~1520 and 1640 cm^{-1} as the metal cation changes from Li^+ to Na^+. Again, the experimental spectrum is best represented by the spectrum calculated for the $Na^+(C_1)$ tautomeric conformation; no evidence for excited tautomeric conformations is observed.

Comparison of the calculated IR spectrum of the first excited tautomeric conformation, $Na^+(C_6)$, to the IRMPD action spectrum suggests that the $Na^+(C_6)$ is not accessed in the experiments as there are several notable differences. The predicted CO stretch is blueshifted to 1655 cm^{-1} and becomes slightly narrower compared with the measured IRMPD band at 1640 cm^{-1}. The measured band at 1460 cm^{-1} is blueshifted by ~50 cm^{-1} and is predicted in much lower intensity in the computed spectrum. The most diagnostic difference indicating the absence of $Na^+(C_6)$ in the experiments is the absence of the

band predicted to occur at 1315 cm^{-1} in the measured IRMPD spectrum. Likewise, the weak IRMPD features observed at 1185, 1340, and 1410 cm^{-1} do not appear in the predicted spectrum. The calculated IR spectrum for the $Na^+(C_3)$ tautomeric conformation exhibits a strong band at ~1640 cm^{-1} that corresponds to NH_2 scissoring coupled with C2–N3 and C5–C6 stretching, which agrees with the most intense band measured at 1640 cm^{-1}. However, redshifting of the CO stretch is much more pronounced because its functionality has changed from keto to enol such that it now appears at 1435 cm^{-1}, which does not have a comparable experimentally observed band. The calculations predict an IR band at 1555 cm^{-1}, whereas no band is observed at this frequency in the measured IRMPD spectrum. The band observed at 1460 cm^{-1} does not have a comparable predicted band in the calculated spectrum for the $Na^+(C_3)$ tautomeric conformation. Based on these comparisons, it is clear that the $Na^+(C_3)$ conformation is also not accessed in the experiments. Thus, the experimental IRMPD spectrum is well represented by that calculated for the ground-state $Na^+(C_1)$ tautomeric conformation; no evidence for the presence of excited tautomeric conformations in the experiments is observed.

Comparison of IRMPD and Theoretical IR Spectra of K^+(cytosine)

Figure 5 shows the measured IRMPD spectrum of the K^+(cytosine) complex compared with theoretical predictions for the three most stable conformations calculated. The appearance of the measured IRMPD spectrum of K^+(cytosine) is similar to that of Na^+(cytosine). However, the most intense band is blueshifted compared with that of the Li^+(cytosine) and Na^+(cytosine) complexes to 1660 cm^{-1}, with a shoulder to the red becoming increasingly obvious. The broad band observed between 1440 and 1520 cm^{-1} for Li^+(cytosine) and Na^+(cytosine) is also partially resolved into two bands. The calculated spectrum of the $K^+(C_1)$ tautomeric conformation correctly predicts the evolution of these spectral features. The appearance of the shoulder to the red becomes increasingly obvious as a result of further redshifting of the band predicted at ~1620 cm^{-1} and blueshifting of the band predicted at ~1640 cm^{-1}. A further blueshifting of the predicted band at ~1520 cm^{-1} results in the split of the broad band located between 1440 and 1520 cm^{-1} in the measured IRMPD spectrum. The IR spectra of the $K^+(C_6)$ and $K^+(C_3)$ tautomeric conformations retain all of the bands that are seen in the lithiated and sodiated tautomeric conformations. Again, the predicted bands at 1315 and 1580 cm^{-1} for the $K^+(C_6)$ conformer, and the bands at 1220, 1430, and 1560 cm^{-1} for the $K^+(C_3)$ conformer, are the most diagnostic bands for these tautomeric conformations. No comparable bands are observed in the measured IRMPD spectrum at these frequencies, indicating that these two low-energy tautomeric conformations are not accessed in the experiments. Additional evidence includes the absence of a predicted band for both $K^+(C_6)$ and $K^+(C_3)$ tautomeric conformations that is comparable with

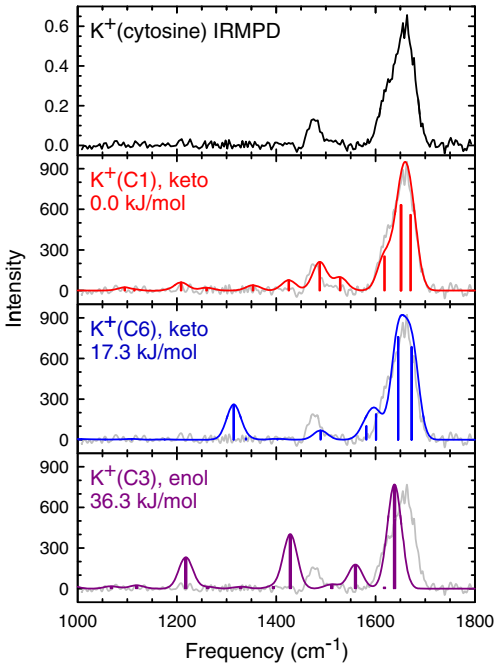

Figure 5. Comparison of the measured IRMPD action spectrum of the K^+(cytosine) complex with IR spectra for the three most stable tautomeric conformations of K^+(cytosine) predicted at the B3LYP/def2-TZVPPD level of theory. For ease of comparison, the IRMPD spectrum, scaled to match the intensity of the most intense spectral feature, is also shown in gray along with each of the theoretical IR spectra

measured IRMPD band at 1470 cm^{-1}, and a redshift in the predicted strong band at 1640 cm^{-1} for the $K^+(C_3)$ tautomeric conformation compared with the measured IRMPD band at 1660 cm^{-1}. Thus, only the ground-state $K^+(C_1)$ conformer is accessed in the experiments.

Comparison of IRMPD and Theoretical IR Spectra of Rb^+(cytosine)

Figure 6 compares the measured IRMPD spectrum of the Rb^+(cytosine) complex with the theoretical linear IR spectra for the three most stable tautomeric conformations calculated. The appearance of the measured IRMPD spectrum of the Rb^+(cytosine) complex is similar to that of the K^+(cytosine) complex, but the S/N is vastly improved such that new features are clearly evident in the measured IRMPD spectrum of the Rb^+(cytosine) complex. The most intense band corresponding to the carbonyl stretch is further blueshifted to 1670 cm^{-1} as a result of the weaker binding of the heavier alkali metal cations to the carbonyl group. The band at 1630 cm^{-1} for the K^+(cytosine) complex is redshifted by 10 cm^{-1} for the Rb^+(cytosine) complex. The shifting of these two bands makes the shoulder to the red of the most intense band increasingly apparent. In addition, it is clear that a new

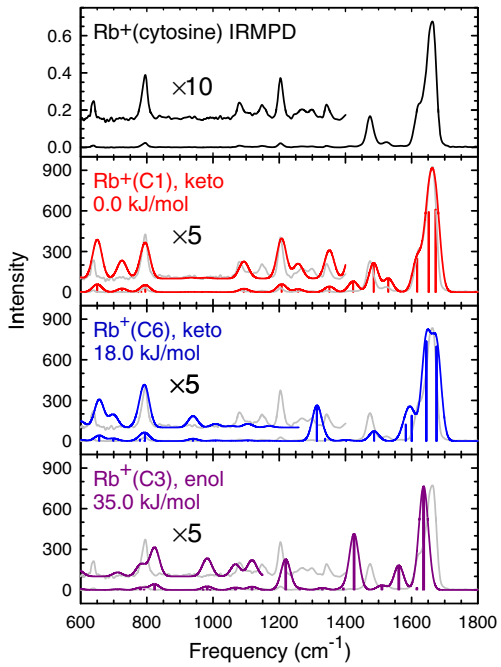

Figure 6. Comparison of the measured IRMPD action spectrum of the Rb^+(cytosine) complex with IR spectra for the three most stable tautomeric conformations of Rb^+(cytosine) predicted at the B3LYP/def2-TZVPPD level of theory. For ease of comparison, the IRMPD spectrum, scaled to match the intensity of the most intense spectral feature, is also shown in gray along with each of the theoretical IR spectra

band at 1520 cm^{-1} appears in the measured IRMPD spectrum for the Rb^+(cytosine) complex. As mentioned in the previous section, this low intensity band at ~1520 cm^{-1} exhibits overlap with the band at ~1480 cm^{-1} for the smaller alkali metal cation-cytosine complexes, producing a broad band between 1440 and 1520 cm^{-1}. As the size of the alkali metal cation increases, the band at 1480 cm^{-1} is increasingly redshifted and the band at 1500 cm^{-1} is increasingly blueshifted. Eventually, the broad band splits into two bands, as seen in the measured IRMPD spectrum for the K^+(cytosine) complex, and becomes easily distinguishable in the spectrum for the Rb^+(cytosine) complex. Weak bands in the region between 600 and 1400 cm^{-1} become increasingly apparent, and are best represented by the spectrum predicted for the $Rb^+(C_1)$ tautomeric conformation. The calculated spectrum of $Rb^+(C_1)$ accurately estimates the shifting in band positions and the new spectral features observed in the measured IRMPD spectrum. The predicted bands at 1315 and 1590 cm^{-1} for the $Rb^+(C_6)$ conformer, and the bands predicted at 1425 and 1555 cm^{-1} for the $Rb^+(C_3)$ conformer are again the most diagnostic bands for these tautomeric conformations. No comparable bands are observed in the measured IRMPD spectrum at these frequencies, indicating that these two low-energy tautomeric conformations are not accessed in the experiments. Additional evidence includes the absence of a predicted band that is comparable to the measured IRMPD band at 1470 cm^{-1} and a redshift of 30 cm^{-1} in the predicted strong band at 1635 cm^{-1} for the $K^+(C_3)$ tautomeric conformation compared with the measured IRMPD band at 1665 cm^{-1}. Thus, the $Rb^+(C_1)$ tautomeric conformation is the only structure accessed in the experiments.

Comparison of IRMPD and Theoretical IR Spectra of Cs^+(cytosine)

A comparison of the measured IRMPD spectrum of the Cs^+(cytosine) complex with theoretical predictions for the three most stable tautomeric conformations calculated can be found in the Supplementary Information, Figure S3. Compared with the measured IRMPD spectrum of the Rb^+(cytosine) complex, all of the bands are retained, but the positions and intensities of these bands continue to evolve with the size of the alkali metal cation. All bands grow in intensity compared with those of the Rb^+(cytosine) complex. The band corresponding to the CO stretch is again observed at ~1670 cm^{-1}, and the shoulder to the red of this band is even more evident in the IRMPD spectrum. Other differences include further redshifting of the band at 1470 cm^{-1} and blueshifting of the band at 1520 cm^{-1} as the metal cation changes from Rb^+ to Cs^+. The calculated spectrum for the $Cs^+(C_1)$ tautomeric conformation correctly predicts the shifting of the major IR bands. The minor features at 640, 720, 800, 1100, 1210, 1260, and 1340 cm^{-1} are also present in the calculated spectrum for $Cs^+(C_1)$. Furthermore, as observed for the other alkali metal cation–cytosine complexes, the diagnostic bands at 1315 cm^{-1} for the $Cs^+(C_6)$ conformer, and the bands at 1435 and 1600 cm^{-1} for the $Cs^+(C_3)$ conformer, are not observed in the measured IRMPD spectrum. Additional evidence includes the absence of a predicted band that is comparable to measured IRMPD band at 1470 cm^{-1} and a redshift of 35 cm^{-1} in the predicted strong band at 1635 cm^{-1} for the $Cs^+(C_3)$ tautomeric conformation compared with the measured IRMPD band at 1670 cm^{-1}. Thus, it is clear that the only tautomeric conformation accessed in the experiments is the $Cs^+(C_1)$ conformer.

Comparison of IRMPD Spectra of the Alkali Metal Cation-Cytosine Complexes to the Protonated Cytosine Complex

The IRMPD action spectra of protonated cytosine, H^+(cytosine) has been reported by Tortajada and coworkers [55]. The appearance of the measured IRMPD spectrum of H^+(cytosine) exhibits both similarities and differences compared with the IRMPD spectra of the alkali metal cation-cytosine complexes. The most intense band for the H^+(cytosine) complex is the band corresponding to NH_2 scissoring at 1645 cm^{-1}, with a shoulder to the red at 1622 cm^{-1}. The CO stretch is redshifted to 1600 cm^{-1}, a shift of 40 cm^{-1} compared with that of the Li^+(cytosine) complex,

a result of the much stronger interaction of the carbonyl group with the proton. The diagnostic band for the alkali metal cation complexes at ~1480 cm^{-1} is also observed in the measured IRMPD spectrum of H^+(cytosine); however, this band is blueshifted to 1502 cm^{-1}. In addition, the band at ~1200 cm^{-1} is present at a higher intensity in the measured IRMPD spectrum of H^+(cytosine) compared with that of the Rb^+(cytosine) and Cs^+(cytosine) complexes. As a proton is a small, singly charged cation, which exhibits similarities to the alkali metal cations, the trends in the shifting of these two bands are consistent with our previous observations, and correlate with the size of the cation. In addition, a band at ~1800 cm^{-1} is observed in the measured IRMPD spectrum of H^+(cytosine), which corresponds to a free C=O stretch. Comparison of the measured IRMPD spectrum to spectra calculated for the enol tautomer C_1_hb (protonation at the carbonyl O atom) and oxo tautomer C_1_hb (protonation at the N3 atom) indicates the presence of both tautomers under their experimental conditions.

Conclusions

The IRMPD action spectra of five M^+(cytosine) complexes, where M^+=Li^+, Na^+, K^+, Rb^+, and Cs^+, were measured using a Fourier transform ion cyclotron resonance mass spectrometer coupled with a free electron laser. The measured IRMPD spectra of all five alkali metal cation–cytosine complexes share similarities, but also exhibit systematic changes in the band positions as a function of the size of the alkali metal cation. Comparisons of the measured IRMPD spectra to linear IR spectra calculated at the B3LYP/def2-TZVPPD level of theory for the three most stable M^+(cytosine) tautomeric conformations, $M^+(C_1)$, $M^+(C_3)$, and $M^+(C_6)$, are made to determine the species accessed under our experimental conditions. In all cases, it is clear that the only tautomeric conformation accessed in the experiments is the bidentate $M^+(C_1)$ tautomeric conformation, in agreement with the predicted ground-state structures for these complexes. The combination of experimental and theoretical results provides insight into the influence of alkali metal cation binding on the relative stabilities of the various tautomeric forms of cytosine. In particular, the very strong binding to the C_1 tautomer compared with the other tautomers ensures that only one tautomeric conformation of the M^+(cytosine) complexes is accessed in the experiments, whereas multiple low-energy tautomers and, in particular C_1, C_2, and C_3, are competitive for neutral cytosine. However, quantitative determination of the strength of the binding in these ground-state alkali metal cation–cytosine complexes remains experimentally elusive. Thus, it would be useful to reexamine the M^+(cytosine) complexes using instrumentation capable of determining thermochemical properties such as a guided ion beam tandem mass spectrometer equipped with an ESI source so that the strength of binding in the ground-state conformers can be accurately determined. These measurements are currently being pursued in a related study.

Acknowledgments

The authors acknowledge financial support for this work by the National Science Foundation, grants OISE-0730072 and CHE-0911191. The authors also like to thank WSU C&IT for computer time. This work is part of the research program of FOM, which is financially supported by the Nederlandse Organisatie voor Wetenschappelijk Onderzoek (NWO). The skillful assistance of the FELIX staff is gratefully acknowledged.

References

1. Crick, F.: Central dogma of molecular biology. *Nature* **227**, 561–563 (1970)
2. Clarke, M.J.: Electrochemistry, synthesis, and spectra of pentaammineruthenium(III) complexes of cytidine, adenosine, and related ligands. *J. Am. Chem. Soc.* **100**, 5068–5075 (1978)
3. Lippert, B., Schöllhorn, H., Thewalt, U.: Metal-stabilized rare tautomers of nucleobases. 1. Iminooxo form of cytosine: formation through metal migration and estimation of the geometry of the free tautomer. *J. Am. Chem. Soc* **108**, 6616–6621 (1986)
4. Pichierri, F., Holthenrich, D., Zangrando, E., Lippert, B., Randaccio, L.: Metal-stabilized rare tautomers of nucleobases 5. Iminooxo tautomer of cytosine coordinated to Pt(II) with metal and nucleobase in *syn* and *anti* orientations. *J. Biol. Inorg. Chem.* **1**, 439–445 (1996)
5. Müller, J., Zangrando, E., Pahlke, N., Freisinger, E., Randaccio, L., Lippert, B.: Affinity of the iminooxo tautomer anion of 1-methylcytosine in trans-$[Pt(NH_3)_2(1\text{-MeC-}N_4)_2]^{2+}$ for heterometals. *Chem. Eur. J.* **4**, 397–405 (1998)
6. Zamora, F., Kunsman, M., Sabat, M., Lippert, B.: Metal-stabilized rare tautomers of nucleobases. 6. Imino tautomer of adenine in a mixed-nucleobase complex of mercury(II). *Inorg. Chem.* **36**, 1583–1587 (1997)
7. Arpalahti, J., Klika, K.D.: Platination of the exocyclic amino group of the adenine nucleobase by Pt(II) migration. *Eur. J. Inorg. Chem.* **8**, 1199–1201 (1999)
8. Day, E.F., Crawford, C.A., Folting, K., Dunbar, K.R., Christon, G.: New metal-binding mode for adenine: A bidentate (N6, N7) bridging mode in the complex [Mo2(O2CCHF2)2(9-EtAH)2(MeCN)2](BF4)2•2MeCN. *J. Am. Chem. Soc.* **116**, 9339–9340 (1994)
9. Velders, A.H., van der Geest, B., Kooijman, H., Spek, A.L., Haasnoot, J.G., Reedijk, J.: Ruthenium(III) coordination to the exocyclic nitrogen of 9-methyladenine and stabilisation of the rare imine tautomer by intramolecular hydrogen bonding. *Eur. J. Inorg. Chem.* 369−372 (2001)
10. Nei, Y.-W., Akinyemi, T.E., Kaczan, C.M., Steill, J.D., Berden, G., Oomens, J., Rodgers, M.T.: Infrared multiple photon dissociation action spectroscopy of sodiated uracil and thiouracils: Effects of thioketo-substitution on gas-phase conformation. *Int. J. Mass Spectrom.* **308**, 191–202 (2011)
11. Yang, Z., Rodgers, M.T.: Tautomerization in the formation and collision-induced dissociation of alkali metal cation-cytosine complexes. *Phys. Chem. Chem. Phys.* **14**, 4517–4526 (2012)
12. Watson, J.D., Crick, F.: Genetical implications of the structure of deoxyribonucleic acid. *Nature* **171**, 964–967 (1953)
13. Topal, M.D., Fresco, J.R.: Complementary base pairing and the origin of substitution mutations. *Nature* **263**, 285–289 (1976)
14. Šponer, J.: J., Hobza, P.: Bifurcated hydrogen bonds in DNA crystal structures. An ab initio quantum chemical study. *J. Am. Chem. Soc.* **116**, 709–714 (1994)
15. Šponer, J., Hobza, P.: Nonplanar geometries of DNA bases. Ab initio second-order Moeller-Plesset study. *J. Phys. Chem.* **98**, 3161–3164 (1994)
16. Hall, R.J., Burton, N.A., Hillier, I.H., Young, P.E.: Tautomeric equilibria in 2-hydroxypyridine and in cytosine. An assessment of density functional methods, including gradient corrections. *Chem. Phys. Lett.* **220**, 129–132 (1994)
17. Sobolewski, A.L., Adamowicz, L.: Theoretical investigations of proton transfer reactions in a hydrogen bonded complex of cytosine with water. *J. Chem. Phys.* **102**, 5708–5718 (1995)

18. Florián, J., Leszczyński, J., Johnson, B.G.: On the intermolecular vibrational modes of the guanine···cytosine, adenine–thymine and formamide–formamide H-bonded dimers. *J. Mol. Struct.* **349**, 421–426 (1995)
19. Fülscher, M.P., Roos, B.O.: Theoretical study of the electronic spectrum of cytosine. *J. Am. Chem. Soc.* **117**, 2089–2095 (1995)
20. Hobza, P., Šponer, J., Polášek, M.: H-bonded and stacked DNA base pairs: Cytosine dimer. An ab initio second-order Moeller-Plesset study. *J. Am. Chem. Soc.* **117**, 792–798 (1995)
21. Colominas, C., Luque, F.J., Orozco, M.: Tautomerism and protonation of guanine and cytosine. Implications in the formation of hydrogen-bonded complexes. *J. Am. Chem. Soc.* **118**, 6811–6821 (1996)
22. Florián, J., Baumruk, V., Leszczyński, J.: IR and Raman spectra, tautomerism, and scaled quantum mechanical force fields of protonated cytosine. *J. Phys. Chem.* **100**, 5578–5589 (1996)
23. Kwiatkowski, J.S., Leszczyński, J.: Molecular structure and vibrational IR spectra of cytosine and its thio and seleno analogues by density functional theory and conventional ab initio calculations. *J. Phys. Chem.* **100**, 941–953 (1996)
24. Fogarasi, G.: High-level electron correlation calculations on some tautomers of cytosine. *J. Mol. Struct.* **413**, 271–278 (1997)
25. Kobayashi, R.: A CCSD(T) study of the relative stabilities of cytosine tautomers. *J. Phys. Chem. A* **102**, 10813–10817 (1998)
26. Russo, N., Toscano, M., Grand, A.: Lithium affinity for DNA and RNA nucleobases. The role of theoretical information in the elucidation of the mass spectrometry data. *J. Phys. Chem. B* **105**, 4735–4741 (2001)
27. Russo, N., Toscano, M., Grand, A.: Bond energies and attachment sites of sodium and potassium cations to DNA and RNA nucleic acid bases in the gas phase. *J. Am. Chem. Soc.* **123**, 10272–10279 (2001)
28. Fogarasi, G.: Relative stabilities of three low-energy tautomers of cytosine: A coupled cluster electron correlation study. *J. Phys. Chem. A* **106**, 1381–1390 (2002)
29. Trygubenko, S.A., Bogdan, T.V., Rueda, M., Orozco, M., Luque, F.J., Šponer, J., Slavíček, P., Hobza, P.: Correlated ab initio study of nucleic acid bases and their tautomers in the gas phase, in a microhydrated environment and in aqueous solution. Part 1. Cytosine. *Phys. Chem. Chem. Phys.* **4**, 4192–4203 (2002)
30. Yang, Z., Rodgers, M.T.: Theoretical studies of the unimolecular and bimolecular tautomerization of cytosine. *Phys. Chem. Chem. Phys* **6**, 2749–2757 (2004)
31. Mazzuca, D., Marino, T., Russo, N., Toscano, M.: A theoretical study on tautomerization processes of dehydrated and monohydrated cytosine. *THEOCHEM.* **811**, 161–167 (2007)
32. Szczesniak, M., Szczepaniak, K., Kwiatkowski, J.S., Kubulat, K., Person, W.B.: Matrix isolation infrared studies of nucleic acid constituents. 5. Experimental matrix-isolation and theoretical ab initio SCF molecular orbital studies of the infrared spectra of cytosine monomers. *J. Am. Chem. Soc.* **110**, 8319–8330 (1988)
33. Brown, R.D., Godfrey, P.D., McNaughton, D., Pierlot, A.P.: Tautomers of cytosine by microwave spectroscopy. *J. Am. Chem. Soc.* **111**, 2308–2310 (1989)
34. Monajjemi, M., Ghiasi, R., Sadjadi, M.A.S.: Metal-stabilized rare tautomers: N4 metalated cytosine ($M=Li^+$, Na^+, K^+, Rb^+ and Cs^+), theoretical views. *Appl. Organometal. Chem.* **17**, 635–640 (2003)
35. Lippert, B., Gupta. D.: Promotion of rare nucleobase tautomers by metal binding. *Dalton Trans*. 4619−4634 (2009)
36. Winter, M.: *WebElements Periodic Table of the Elements | Cesium | biological information*, WebElements (2012)
37. Valle, J.J., Eyler, J.R., Oomens, J., Moore, D.T., van der Meer, A.F.G., von Helden, G., Meijer, G., Hendrickson, C.L., Marshall, A.G., Blakney, G.T.: Free electron laser-Fourier transform ion cyclotron resonance mass spectrometry facility for obtaining infrared multiphoton dissociation spectra of gaseous ions. *Rev. Sci. Instrum.* **76**, 023103–7 (2005)
38. Polfer, N.C., Oomens, J., Moore, D.T., von Helden, G., Meijer, G., Dunbar, R.C.: Infrared spectroscopy of phenylalanine Ag(I) and Zn(II) complexes in the gas phase. *J. Am. Chem. Soc.* **128**, 517–525 (2006)
39. Polfer, N.C., Oomens, J.: Reaction products in mass spectrometry elucidated with infrared spectroscopy. *Phys. Chem. Chem. Phys* **9**, 3804–3817 (2007)
40. Frisch, M.J., Trucks, G.W., Schlegel, H.B., Scuseria, G.E., Robb, M.A., Cheeseman, J.R., Montgomery Jr., J.A., Vreven, T., Kudin, K.N., Burant, J.C., Millam, J.M., Iyengar, S.S., Tomasi, J., Barone, V., Mennucci, B., Cossi, M., Scalmani, G., Rega, N., Petersson, G.A., Nakatsuji, H., Hada, M., Ehara, M., Toyota, K., Fukuda, R., Hasegawa, J., Ishida, M., Nakajima, T., Honda, Y., Kitao, O., Nakai, H., Klene, M., Li, X., Knox, J.E., Hratchian, H.P., Cross, J.B., Bakken, V., Adamo, C., Jaramillo, J., Gomperts, R., Stratmann, R.E., Yazyev, O., Austin, A.J., Cammi, R., Pomelli, C., Ochterski, J.W., Ayala, P.Y., Morokuma, K., Voth, G.A., Salvador, P., Dannenberg, J.J., Zakrzewski, V.G., Dapprich, S., Daniels, A.D., Strain, M.C., Farkas, O., Malick, D.K., Rabuck, A.D., Raghavachari, K., Foresman, J.B., Ortiz, J.V., Cui, Q., Baboul, A.G., Clifford, S., Cioslowski, J., Stefanov, B.B., Liu, G., Liashenko, A., Piskorz, P., Komaromi, I., Martin, R.L., Fox, D.J., Keith, T., Al-Laham, M.A., Peng, C.Y., Nanayakkara, A., Challacombe, M., Gill, P.M.W., Johnson, B., Chen, W., Wong, M.W., Gonzalez, C., Pople, J.A.: Gaussian 03, Revision C.02. Gaussian, Inc, Wallingford (2004)
41. Foresman, J.B., Frisch, Æ.:*Exploring Chemistry with Electronic Structures Methods*, 2nd ed.; Gaussian: Pittsburg, 1996, p. 64.
42. Pople, J.A., Scott, A.P., Wong, M.W., Radom, L.: Scaling Factors for Obtaining Fundamental Vibrational Frequencies and Zero-Point Energies from HF/6-31G* and MP2/6-31G* Harmonic Frequencies. *Isr. J. Chem. Soc.* **33**, 345–350 (1993)
43. Frisch, M.J., Trucks, G.W., Schlegel, H.B., Scuseria, G.E., Robb, M.A., Cheeseman, J.R., Scalmani, G., Barone, V., Mennucci, B., Petersson, G.A., Nakatsuji, H., Caricato, M., Li, X., Hratchian, H.P., Izmaylov, A.F., Bloino, J., Zheng, G., Sonnenberg, J.L., Hada, M., Ehara, M., Toyota, K., Fukuda, R., Hasegawa, J., Ishida, M., Nakajima, T., Honda, Y., Kitao, O., Nakai, H., Vreven, T., Montgomery Jr., J.A., Peralta, J.E., Ogliaro, F., Bearpark, M., Heyd, J.J., Brothers, E., Kudin, K.N., Staroverov, V.N., Kobayashi, R., Normand, J., Raghavachari, K., Rendell, A., Burant, J.C., Iyengar, S.S., Tomasi, J., Cossi, M., Rega, N., Millam, J.M., Klene, M., Knox, J.E., Cross, J.B., Bakken, V., Adamo, C., Jaramillo, J., Gomperts, R., Stratmann, R.E., Yazyev, O., Austin, A.J., Cammi, R., Pomelli, C., Ochterski, J.W., Martin, R.L., Morokuma, K., Zakrzewski, V.G., Voth, G.A., Salvador, P., Dannenberg, J.J., Dapprich, S., Daniels, A.D., Farkas, O., Foresman, J.B., Ortiz, J.V., Cioslowski, J., Fox, D.J.: Gaussian 09, Revision A.1. Gaussian, Inc, Wallingford (2009)
44. Weigend, F., Ahlrichs, R.: Balanced basis sets of split valence, triple zeta valence and quadruple zeta valence quality for H to Rn: Design and assessment of accuracy. *Phys. Chem. Chem. Phys* **7**, 3297–3305 (2005)
45. Leininger, T., Nicklass, A., Kuechle, W., Stoll, H., Dolg, M., Bergner, A.: The accuracy of the pseudopotential approximation: Non-frozen-core effects for spectroscopic constants of alkali fluorides XF (X=K, Rb, Cs). *Chem. Phys. Lett.* **255**, 274–280 (1996)
46. Feller, D.: The role of databases in support of computational chemistry calculations. *J. Comp. Chem.* **17**, 1571–1586 (1996)
47. Schuchardt, K.L., Didier, B.T., Elsethagen, T., Sun, L., Gurumoorthi, V., Chase, J., Li, J., Windus, T.L.: Basis set exchange: A community database for computational sciences. *J. Chem. Inf. Model.* **47**, 1045–1052 (2007)
48. Armentrout, P.B., Chen, Y., Rodgers, M.T.: Metal cation dependence of interactions with amino acids: Bond energies of Cs^+ to Gly, Pro, Ser, Thr, and Cys. *J. Phys. Chem. A* **116**, 3989–3999 (2012)
49. McLean, A.D., Chandler, G.S.: Contracted Gaussian basis sets for molecular calculations. I. Second row atoms, z = 11–18. *J. Chem. Phys.* **72**, 5639–5648 (1980)
50. Hay, P.J., Wadt, W.R.: Ab initio effective core potentials for molecular calculations. Potentials for K to Au including the outermost core orbitals. *J. Chem. Phys*. **82**, 299–310 (1985)
51. Glendening, E.D., Feller, D., Thompson, M.A.: An ab initio investigation of the structure and alkali metal cation selectivity of 18-crown-6. *J. Am. Chem. Soc.* **116**, 10657–10669 (1994)
52. Rodgers, M.T., Armentrout, P.B.: A critical evaluation of the experimental and theoretical determination of lithium cation affinities. *Int. J. Mass Spectrom.* **267**, 167–182 (2007)
53. Armentrout, P.B., Austin, C.A., Rodgers, M.T.: Alkali metal cation interactions with 12-crown-4 in the gas phase: Revisited. *Int. J. Mass Spectrom*. **330/332**, 16–26 (2012)
54. Wilson, R.G., Brewer, G.R.: Ion Beams with Applications to Ion Implantation. Wiley, New York (1973)
55. Salpin, J.-Y., Guillaumount, S., Tortajada, J., MacAleese, L., Lemaire, J., Maitre, P.: Infrared spectra of protonated uracil, thymine and cytosine. *Chem. Phys. Chem.* **8**, 2235–2244 (2007)